

Modeling Return Periods of Tropical Cyclone Intensities in the Vicinity of Hawaii*

PAO-SHIN CHU AND JIANXIN WANG

Department of Meteorology, School of Ocean and Earth Science and Technology, University of Hawaii at Manoa, Honolulu, Hawaii

(Manuscript received 29 September 1997, in final form 5 January 1998)

ABSTRACT

Tropical cyclones in the vicinity of Hawaii have resulted in great property damage. An estimate of the return periods of tropical cyclone intensities is of particular interest to governments, public interest groups, and private sectors.

A dimensionless quantity called relative intensity (RI) is used to combine all available information about the tropical cyclone characteristics at different places and times. To make a satisfactory estimate of the return periods of tropical cyclone intensities, a large number of RIs are simulated by the Monte Carlo method based on the extreme value distribution. The return periods of RIs and the corresponding maximum wind speeds associated with tropical cyclones are then estimated by combining the information about the intensities and occurrences. Results show that the return periods of maximum wind speeds equal to or greater than 125, 110, 100, 80, 64, 50, and 34 kt are estimated to be 137, 59, 33, 12, 6.6, 4, and 3.2 years, respectively.

The Monte Carlo method is also used to estimate the confidence intervals of the return periods of tropical cyclone intensities. The sensitivity test is conducted by removing the portion of the data prior to satellite observations. For maximum wind speeds less than 80 kt, estimates of return periods from the shorter dataset (1970–95) are almost identical to those when the complete duration time series are used (1949–95).

1. Introduction

The tropical cyclone is one of the most destructive natural disasters that cause loss of lives and enormous property damage around the world every year. Climate information about tropical cyclones is thus useful for decision makers in many fields (e.g., coastal zone management, civil defense, insurance, and power utilities). For this information to be useful, an analysis of climate risks in a region, which involves extreme events, is needed (Neumann 1987).

The return period of maximum wind speeds associated with tropical cyclones refers to the average period in which an event is expected to recur once. This information is used for building purposes and disaster preparedness. Building codes in the U.S. mainland are often set to accommodate the 100-yr extreme events. Methods for estimating return periods of tropical cyclones have been proposed by Russell (1971), Batts et al. (1980), Georgiou (1985), Neumann (1987), Darling (1991), and Rupp and Lander (1996), among others. The

Gumbel distribution, in essence, a double exponential distribution, is one of the most frequently used models because of its simplicity and wide applicability (e.g., Gumbel 1958; Ramage 1995). Rupp and Lander (1996) apply the Gumbel method to estimate the return periods of the cyclone-related extreme winds for Guam.

The computer simulation method for assessing long-term risk levels associated with tropical cyclones has emerged as a powerful tool and has frequently been used. This method was first suggested by Russell (1971) and later applied and developed by other researchers (Batts 1980; Georgiou 1985; Neumann 1987). These studies are similar in overall strategy, although they differ in almost every detail. An extreme value distribution (EVD) is selected and fit to central pressures or maximum wind speeds of tropical cyclones coming close to a site. Then a sequence of tropical cyclones is simulated from this distribution using the Monte Carlo method. Local occurrences of tropical cyclones are taken into account. Thus, the probability of the annual occurrences for a given maximum wind speed associated with tropical cyclones is obtained.

Darling (1991) presents a rather sophisticated approach to estimate the probability of exceeding a given wind speed in one year at any site in the tropical Atlantic basin. The relative intensity (RI) of a tropical cyclone at any site in time is first defined. The empirical distribution of the RIs as a function of time is then derived from all the Atlantic tropical cyclone data. Combining the empirical distribution with the distribution of time

* School of Ocean and Earth Science and Technology Contribution Number 4650.

Corresponding author address: Dr. Pao-Shin Chu, Department of Meteorology, 2525 Correa Road, University of Hawaii, Honolulu, HI 96822.
E-mail: chu@soest.hawaii.edu

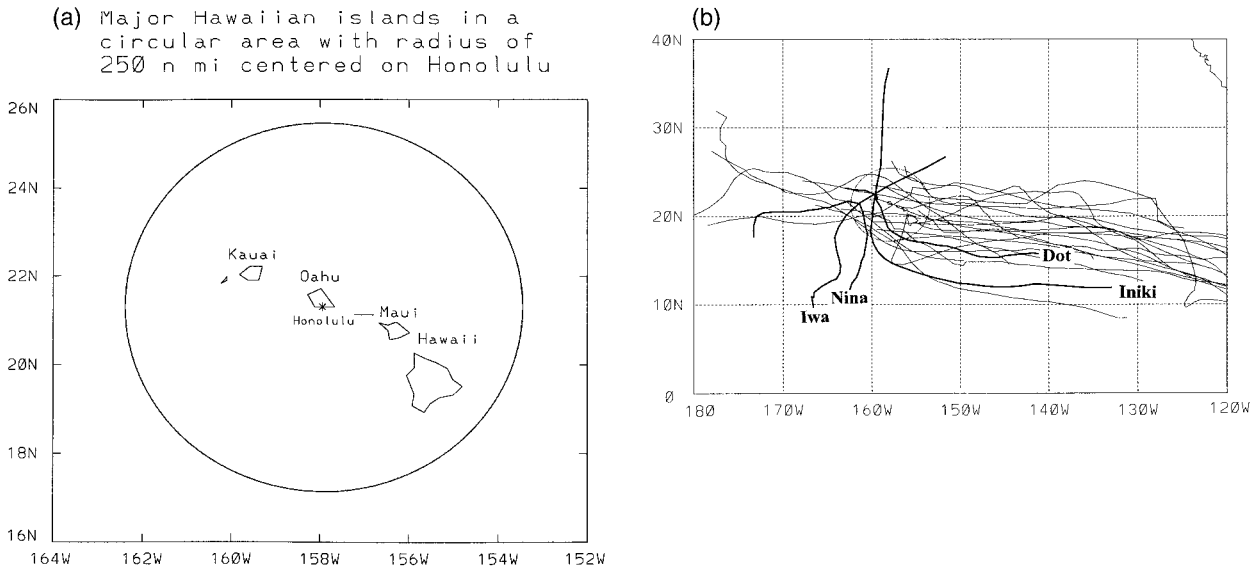


FIG. 1. (a) Map of the major Hawaiian islands and the scan radius of 250 n mi from Honolulu. (b) Tracks of tropical cyclones in the northeast and north-central Pacific that passed within the scan circle from 1949 to 1995. Tracks of Hurricanes Nina (November–December 1957), Dot (August 1959), Iwa (November 1982), and Iniki (September 1992) are denoted as heavy lines.

from tropical cyclone inception to closest approach to a site and other steps, the probabilities and return periods of the maximum wind speeds at the site are obtained. For example, the probability of exceeding 100 kt in one year at Turkey Point in Biscayne Bay, Florida, is 0.004.

Most of the previous studies are concerned with the probabilities of the maximum wind speeds at one specific location on the east coast of the United States or in other regions.

In this study, the return periods of tropical cyclone intensities in the vicinity of Hawaii are estimated from historical tropical cyclone data described in section 2. In section 3, relative intensities are defined and used to assemble and combine all available information about the tropical cyclone characteristics at different places and times. The methodology and computational procedures in simulating and estimating return periods of cyclone intensities are presented in section 4, and in section 5 a sensitivity test of the results presented in section 4 is described. Finally, a summary is given in section 6.

2. Data

a. Data sources

Three datasets are used in this research.

- 1) Tropical cyclone data are supplied by the National Hurricane Center (NHC) in Miami, Florida. This dataset contains measurements of latitudes, longitudes, 1-min sustained maximum wind speeds and, for some recent data, central pressures at 6-h intervals for all 652 tropical cyclones from 1949 to 1995 in the northeast and north-central Pacific (north of the

equator and east of the date line). Landsea and Gray (1992) used a similar dataset from the NHC to study relationships between western Sahelian rainfall and Atlantic hurricanes. Tropical cyclones here refer to tropical storms and hurricanes.

- 2) Monthly global stratospheric (100 hPa) temperatures from 1985 to 1994 are produced by the European Centre for Medium-Range Weather Forecasts. The climatological mean seasonal temperatures in the Northern Hemisphere are calculated from this dataset.
- 3) Monthly mean sea surface temperatures (SSTs) in the Pacific from 1955 to 1995 are supplied by the National Centers for Environmental Prediction (He and Barnston 1996). The SST dataset has a resolution of 10° latitude by 10° longitude. The climatological mean seasonal SSTs are calculated from this dataset.

b. Tropical cyclones in the vicinity of Hawaii

Over the northeast and north-central Pacific basins 652 tropical cyclones have been observed from 1949 to 1995. The average annual occurrence rate is about 13.9. However, the occurrence of tropical cyclones at a specific site in a given year is very small. Therefore, the analysis of tropical cyclones for a specific site must also consider tropical cyclones that pass at some distance from the site. The distance from the site is referred to as a scan radius. In this study, all the tropical cyclones are searched in a scan radius of 250 n mi from Honolulu (Fig. 1a). This scan circle encompasses all the major Hawaiian Islands. In total there are 26 tropical cyclones within this scan circle from 1949 to 1995 (Table 1). Some tropical cyclones passed through this scan circle

TABLE 1. Tropical cyclones within 250 n mi of Honolulu from 1949 to 1995. The relative intensities refer to the strongest stage when a tropical cyclone is in the scan circle.

| Name | Life period | RI |
|-----------|-------------------|-------|
| Hiki | 12–21 Aug 1950 | 0.519 |
| Kanoa | 15–26 Jul 1957 | 0.460 |
| Della | 1–12 Sep 1957 | 0.235 |
| Nina | 29 Nov–6 Dec 1957 | 0.478 |
| Not named | 7–9 Aug 1958 | 0.272 |
| Dot | 1–8 Aug 1959 | 0.895 |
| Irah | 12–21 Sep 1963 | 0.158 |
| Maggie | 20–27 Aug 1970 | 0.272 |
| Diana | 11–20 Aug 1972 | 0.389 |
| Fernanda | 20 Aug–1 Sep 1972 | 0.283 |
| Gwen | 5–18 Aug 1976 | 0.166 |
| Fico | 9–28 Jul 1978 | 0.765 |
| Kay | 16–30 Sep 1980 | 0.180 |
| Jova | 14–21 Sep 1981 | 0.180 |
| Daniel | 7–22 Jul 1982 | 0.166 |
| Gilma | 26 Jul–2 Aug 1982 | 0.166 |
| Iwa | 19–25 Nov 1982 | 0.489 |
| Gil | 23 Jul–5 Aug 1983 | 0.225 |
| Raymond | 8–20 Oct 1983 | 0.169 |
| Gilma | 28 Jul–3 Aug 1988 | 0.154 |
| Dalilia | 11–20 Jul 1989 | 0.330 |
| Fefa | 29 Jul–8 Aug 1991 | 0.178 |
| Orlene | 2–14 Sep 1992 | 0.147 |
| Iniki | 5–13 Sep 1992 | 0.942 |
| Eugene | 15–25 Jul 1993 | 0.166 |
| Emilia | 16–25 Jul 1994 | 0.389 |

while maintaining strength, but others weakened within the scan circle.

Figure 1b displays the tracks of these 26 cyclones in the northeast and north-central Pacific. Nina (29 November–6 December 1957), Dot (1–8 August 1959), Iwa (19–25 November 1982), and Iniki (5–13 September 1992) are four hurricanes that had major impacts on Hawaii. Iniki, by far the strongest one, caused \$2–\$3 billion of damage to Hawaii due to its strong winds, coastal surge, and wave action (Chu and Wang 1997).

3. Relative intensities of tropical cyclones

a. Definition of relative intensities

According to Emanuel (1988a,b), a tropical cyclone can be seen as a heat engine whose total mechanical energy is given by the difference between the sea surface and stratospheric temperatures. One wants to factor out all the related variables by converting them into the dimensionless RI. Following Darling, RI is written as (1), which is the actual central pressure drop divided by the maximum possible pressure drop that the mean seasonal climate allows (Darling 1991):

$$RI = \frac{P_{da} - P_d}{P_{da} - P_{dc}}, \quad (1)$$

where P_{da} denotes surface value of the partial pressure of ambient dry air, given by

$$P_{da} = 1017 - RHe_s.$$

Here, 1017 hPa is the ambient surface pressure in the central North Pacific, which is usually dominated by the sprawling subtropical high pressure system (Rosendal and Shaw 1982). The relative humidity (RH) of ambient air is measured as 81.5% from the observed TAO (Tropical Atmosphere Ocean) data in the equatorial Pacific Ocean (Zhang et al. 1995). The saturation vapor pressure e_s can be computed from the Clausius–Clapeyron equation.

Since the surface air at the center of a tropical cyclone is almost saturated (Jordan 1961), the partial pressure for dry air in the center of a tropical cyclone, P_d , is $P_d = P_c - e_s$. Here, P_c is the central pressure of a tropical cyclone. Referring to (1), the minimum sustainable surface central pressure (of dry air) for a tropical cyclone under the climatic condition is P_{dc} given by $P_{dc} = xP_{da}$ (Emanuel 1988b). The coefficient x is computed from a nonlinear formula as $\ln x = -A(1/x - B)$. Ignoring small contributions from other terms, quantities A and B are functions of the mean seasonal SST T_s , 100-hPa temperature T_0 , e_s , RH, and P_{da} as follows:

$$A \equiv \frac{\epsilon L_v e_s}{(1 - \epsilon)R_v T_s P_{da}},$$

$$B \equiv RH \left[1 + \frac{e_s \ln(RH)}{P_{da} A} \right],$$

where $R_v = 461 \text{ J (kg K)}^{-1}$ is the gas constant of water vapor. Here, $\epsilon = (T_s - T_0)/T_s$ denotes the efficiency of the tropical cyclone as a heat engine.

Equation (1) can be further written as

$$RI = \frac{1017 - P_c + (1 - RH)e_s}{(1 - x)[1017 - (RH \times e_s)]}. \quad (2)$$

b. Computation and discussion of relative intensities

For tropical cyclones where the central pressures are available (post-1988), the RIs can be computed directly from the central pressures at 6-h intervals on the tracks by using (2). When the central pressures are not available (pre-1988), they can be reconstructed from the maximum wind speeds, translational speeds, and latitudes of tropical cyclones, as explained below. Then the RIs can be computed from the reconstructed central pressures by using (2).

According to Willoughby (1990), the gradient wind balance approximately holds in the eyewall region of a tropical cyclone, which can be expressed as a two-variable nonlinear regression model (Darling 1991). With a slight modification, this balance is shown as

$$V_{gr} = a_0 + a_1(1017 - P_c)^{0.5} + a_2 N. \quad (3)$$

In (3), N is the latitude of a tropical cyclone center; a_0 , a_1 , and a_2 are the regression coefficients; V_{gr} is the gradient wind given by (Schwerdt et al. 1979)

$$V_{gr} = V_{max} - 1.5S^{0.63}, \quad (4)$$

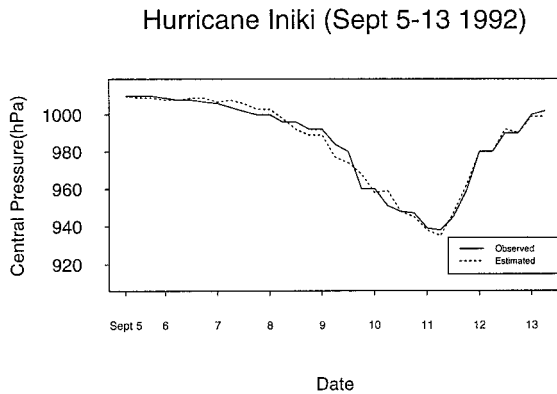


FIG. 2. Time series of the observed and estimated central pressures during Hurricane Iniki. The solid lines are observed pressures and dashed lines are estimated pressures (in hPa).

where V_{max} is the maximum wind speed, available from the tropical cyclone data. Here, S is the translational speed of a tropical cyclone, as estimated from the latitude and longitude measurements of the tropical cyclone center at 6-h intervals. Since the wind field near the center of a tropical cyclone is asymmetric due to the interaction between the rotational effect of the wind and the translational motion of the entire tropical cyclone envelope, the maximum wind usually occurs on the right side of a tropical cyclone (looking in the direction of the translational motion). Thus, an asymmetry factor of $1.5S^{0.63}$ should be subtracted from V_{max} to obtain the gradient wind V_{gr} in (4).

From all 3949 available central pressure and position records in the entire northeast and north-central Pacific, the coefficients in (3) can be estimated by the least squares method as $a_0 = -20.76$, $a_1 = 15.16$, and $a_2 = -0.08$. The multiple correlation coefficient of (3) is 0.98, suggesting the regression fit is very good. The F test shows that the entire regression result of (3) is significant at the 1% test level.

Reversing (3), the central pressure can be estimated as

$$P_c = 1017 - \left(\frac{V_{gr} + 0.08N + 20.76}{15.16} \right)^2 \quad (5)$$

To evaluate the estimation results of (5), all the central pressures from 1949 to 1995 are reconstructed using (5). For all the available observed central pressures, the average absolute error between the observed and fitted central pressures is 2.12 hPa. Here, the observed central pressures are those that are available from the tropical cyclone data. Figure 2 shows the observed (solid line) and estimated (dashed line) central pressures for Hurricane Iniki (5–13 September 1992). The dashed and solid lines are very close to each other. The overall fitting appears to be reasonable.

Then (2) is used to calculate RIs from the reconstructed central pressures. Figure 3 portrays the time history of RIs for Hurricane Iniki. The RI of Iniki

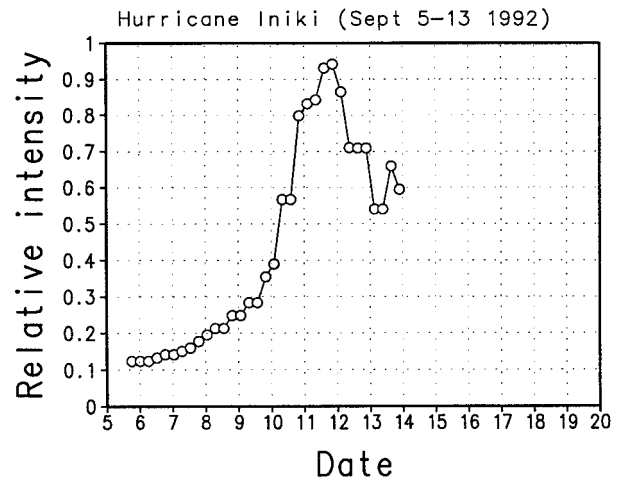


FIG. 3. Time series of the relative intensities during Hurricane Iniki.

reached its maximum value of 0.942 at 1800 (HST) on 11 September 1992, shortly after it made landfall on Kauai (Fig. 1a). Usually the RI values vary between 0 and 1. For a very few tropical cyclones, the RIs can be greater than 1, presumably because the partial pressure for dry air at the center of a tropical cyclone (P_d) is less than the minimum partial central pressure for dry air of a tropical cyclone under climatic conditions (P_{dc}). This may occur when cyclones move northward over colder waters; they will not immediately be in equilibrium with the underlying SSTs and therefore will have an RI exceeding 1 for a limited time period.

4. Methodology and computational procedures

a. A preliminary estimate of the return periods of tropical cyclone intensities

A number of possible distributions can be used to estimate the probabilities of tropical cyclones. For instance, the Poisson distribution is frequently used and its appropriateness has been well demonstrated (Batts et al. 1980; Georgiou 1985; Neumann 1987). A Poisson process should have the following characteristics: 1) The event can have only dichotomous outcomes—occurrence or nonoccurrence, 2) individual events are independent, 3) events occur randomly but at an approximately constant average rate, and 4) events should be rare enough so that the probability of two or more occurring simultaneously is very small.

The annual occurrences of tropical cyclones in the vicinity of Hawaii meet the above characteristics and thus can be well represented by the Poisson process. Let the probability that t tropical cyclones will occur in one year be denoted by $Pr(t)$:

$$Pr(t) = \mu^t \exp(-\mu)/t! \quad (6)$$

where μ specifies the average tropical cyclone occurrence rate per year. In this study, $\mu = 0.5532$ as 26

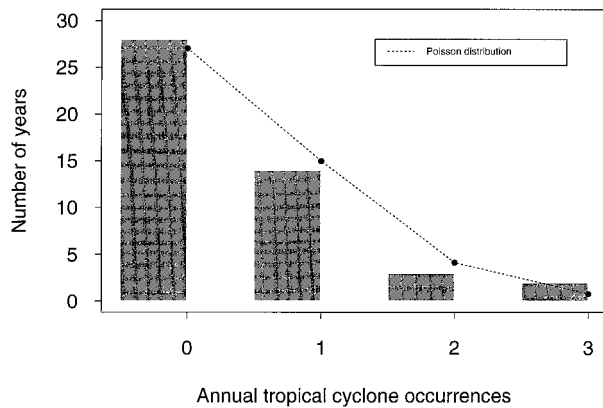


FIG. 4. Histogram of annual tropical cyclone occurrences in the vicinity of Hawaii from 1949 to 1995 (solid bars) and fitted Poisson distribution with $\mu = 0.5532$ occurrence per year (dashed line).

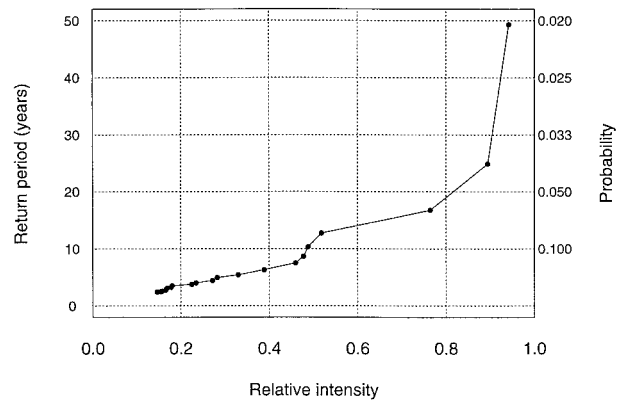


FIG. 5. Estimation of return periods for maximum relative intensities associated with each of the tropical cyclones from 1949 to 1995. The left and right ordinates denote return periods and the corresponding probabilities for the relative intensities of tropical cyclones having at least specified intensity shown in the abscissa.

tropical cyclones occurred in 47 years from 1949 to 1995 in the vicinity of Hawaii.

Figure 4 shows the histogram of the annual tropical cyclone occurrences, superimposed with the fitted Poisson distribution (dashed line) with $\mu = 0.5532$ occurrence per year. There are 28 years with no tropical cyclone occurrence, 14 years with one occurrence, 3 years with two occurrences, and 2 years with three occurrences. The Poisson distribution provides a reasonable representation of the tropical cyclone occurrences. However, the Poisson distribution deals with the tropical cyclone occurrences, but not with the tropical cyclone intensities. To estimate the probabilities of the tropical cyclones with different intensities, the information about intensities and occurrences is combined as follows.

Let F_i denote the probability that a maximum relative intensity X in any one tropical cyclone in the scan circle is less than a value x :

$$F_i = i/(n + 1), \tag{7}$$

where i is the rank of a set of n (here $n = 26$) maximum relative intensities. The probability that the largest X in t tropical cyclones that is less than x can be written as

$$\Pr(X < x | t) = F_i^t. \tag{8}$$

The probability that X is less than x in one year can be denoted as

$$\Pr(X < x) = \sum_{t=0}^{\infty} \Pr(X < x | t) \Pr(t). \tag{9}$$

Substituting (6) and (8) into (9), one obtains

$$\Pr(X < x) = \exp[-\mu(1 - F_i)]. \tag{10}$$

Using (7), (10) can be rewritten as

$$\Pr(X < x) = \exp\{-\mu[1 - i/(n + 1)]\}. \tag{11}$$

The return period $X \geq x$ can be estimated as

$$T = 1/[1 - \Pr(X < x)]. \tag{12}$$

Using (11) and (12), Fig. 5 shows the estimated return periods and probabilities for the maximum RIs associated with each of these 26 tropical cyclones within the scan circle of 250 n mi from Honolulu. The return period for a possible tropical cyclone that is equal to or exceeds Hurricane Iniki's intensity is 49 years; Dot, 25 years; Iwa, 10 years; and Nina, 8.6 years. The return periods for most other tropical cyclones are less than 10 years.

There are large gaps among the strong RIs (e.g., 0.52–0.77) in Fig. 5. Because the occurrences of these strong tropical cyclones are rare, an accurate estimate of the return periods of these tropical cyclones is difficult from the few available cases. Moreover, it is impossible to estimate the return periods for potentially strong tropical cyclones that are beyond the range of the observations. Thus, a variety of tropical cyclone intensities is simulated by the Monte Carlo method based on the extreme value distribution.

b. Extreme value distributions (EVDs)

The relative intensities are positively skewed and nonnegative. It is natural to use some positively skewed EVDs to describe RIs. Among them, the most well-known distributions are the Gumbel, Weibull, and log-normal distributions. Recently, Brown and Katz (1995) applied EVDs to daily maximum and minimum temperature time series in the U.S. midwest and southeast. In the following description, $f(x)$ denotes the probability density function (pdf), $F(x)$ the cumulative distribution function (CDF), X the random variable of the relative intensity, and x is a possible value of X .

1) THEORETICAL DISTRIBUTIONS

(i) Gumbel distribution

The Gumbel distribution is also known as the type I EVD, and its pdf is

$$f(x) = (1/\beta) \exp\{-\exp[-(x - \xi)/\beta] - (x - \xi)/\beta\}. \tag{13}$$

The CDF can be obtained as

$$F(x) = \exp\{-\exp[-(x - \xi)/\beta]\}, \tag{14}$$

where ξ and β are location and scale parameters, respectively. The Gumbel pdf is positively skewed and has its maximum at $x = \xi$. The moment estimators for the Gumbel distribution parameters are $\beta = \sigma 6^{0.5}/\pi = 0.1787$ and $\xi = \bar{x} - 0.57721\beta = 0.2343$. It is also possible to estimate β and ξ from other methods, but Lowery and Nash (1970) concluded that the method of moment is just as satisfactory as other methods.

(ii) Weibull distribution

The Weibull distribution is known as the type III EVI and its pdf is

$$f(x) = (\alpha/\beta)(x/\beta)^{\alpha-1} \exp[-(x/\beta)^\alpha], \tag{15}$$

$x, \alpha, \beta > 0.$

The CDF can be obtained as

$$F(x) = \Pr\{X < x\} = 1 - \exp[-(x/\beta)^\alpha]. \tag{16}$$

The two parameters α and β are called the shape and scale parameters, respectively. Using the method of maximum likelihood, α and β can be obtained as $\alpha = 1.6585$ and $\beta = 0.3815$.

(iii) Lognormal distribution

The lognormal distribution is also chosen here because the parent distribution of the extreme value frequently comes from the lognormal, particularly when the largest extreme value is considered (Haan 1977). One can make a transformation $Y = \ln(X)$ ($X > 0$). If X follows the lognormal distribution, the transformed variable Y follows the Gaussian or normal distribution with the pdf:

$$f(y) = \frac{1}{\sigma(2\pi)^{0.5}} \exp[-(y - \mu)^2/(2\sigma^2)], \tag{17}$$

where the two parameters μ and σ are the mean and standard deviation, respectively, of the transformed variable Y . In this study, $\mu = -1.2645$ and $\sigma = 0.5804$.

Because analytic integration of (17) is impossible, the formula for CDF, $F(y)$, corresponding to (17), does not exist. The CDF can be obtained by numerical integration.

2) GOODNESS OF FIT

As long as the parameters are fitted, the theoretical pdf and CDF can be calculated, as discussed above. The empirical CDF can be estimated from the RI data in Table 1. Let

$$F_n(x_{(i)}) = i/(n + 1). \tag{18}$$

Here $i = 1, 2, \dots, n$ denotes the rank of the relative intensity $x_{(i)}$ in ascending order and $n = 26$.

The quantile-quantile ($Q-Q$) plot is a probability plot comparing the observed RIs and the fitted RIs. The observed RIs are calculated from (2). The fitted RIs can be obtained from the reversed theoretical CDF,

$$x'_{(i)} = F^{-1}[i/(n + 1)]. \tag{19}$$

Each plotted point in a $Q-Q$ plot has a Cartesian coordinate $(x_{(i)}, x'_{(i)})$. As an example, Fig. 6 shows the histogram, pdf, CDF, and $Q-Q$ plot for the lognormal distribution. To assess the goodness of fit, the histogram is compared with the pdf, empirical CDF with theoretical CDF, and observed RIs with fitted RIs for the lognormal distribution. Clearly, the best distribution will exhibit the least difference between the histogram and pdf, empirical CDF and theoretical CDF, and the observed RIs and fitted RIs. In the CDF panel, the solid and dashed lines are close for the lognormal distribution. In the $Q-Q$ plot, the dots are near the straight line except for a very few cases. Visually, the observed RIs follow the lognormal distribution quite well, although the three strongest RIs tend to be underestimated. Similar results can be obtained from the Weibull and Gumbel distributions (not shown).

The Kolmogorov-Smirnov (K-S) test is frequently used in quantitative tests of the goodness of fit. Originally, the K-S test was applicable to any theoretical distributions, provided that the parameters have not been estimated from the data batch. This provision seriously limits the use of the K-S test.

Lilliefors modified the original K-S test so that it can be used in situations where the parameters have been fitted to the sample data (Wilks 1995). The modified K-S test is often called the Lilliefors test. The statistic for the Lilliefors test is the same as that used in the original K-S test, which is the absolute value of the largest difference (D) between the theoretical and empirical CDFs,

$$D = \max_x |F_n(x) - F(x)|, \tag{20}$$

where $F(x)$ is the theoretical CDF for the distribution of interests. Here, $F_n(x)$ is the empirical CDF, as given by (18). If a sufficiently large discrepancy is obtained, in an absolute value sense, the modified K-S test rejects the null hypothesis at a specified level of significance. The D values for the three distributions are given in Table 2. Under the 5% test level, the hypotheses of the Gumbel, Weibull, and lognormal distributions cannot be rejected. Therefore, each of these three distributions can well describe the relative intensities. Among them, the Weibull distribution appears to be best because of its smallest D value.

However, the Lilliefors test is only based on the largest difference between the empirical and theoretical CDFs at one sample point. It is more reasonable to use the average difference between the empirical and the-

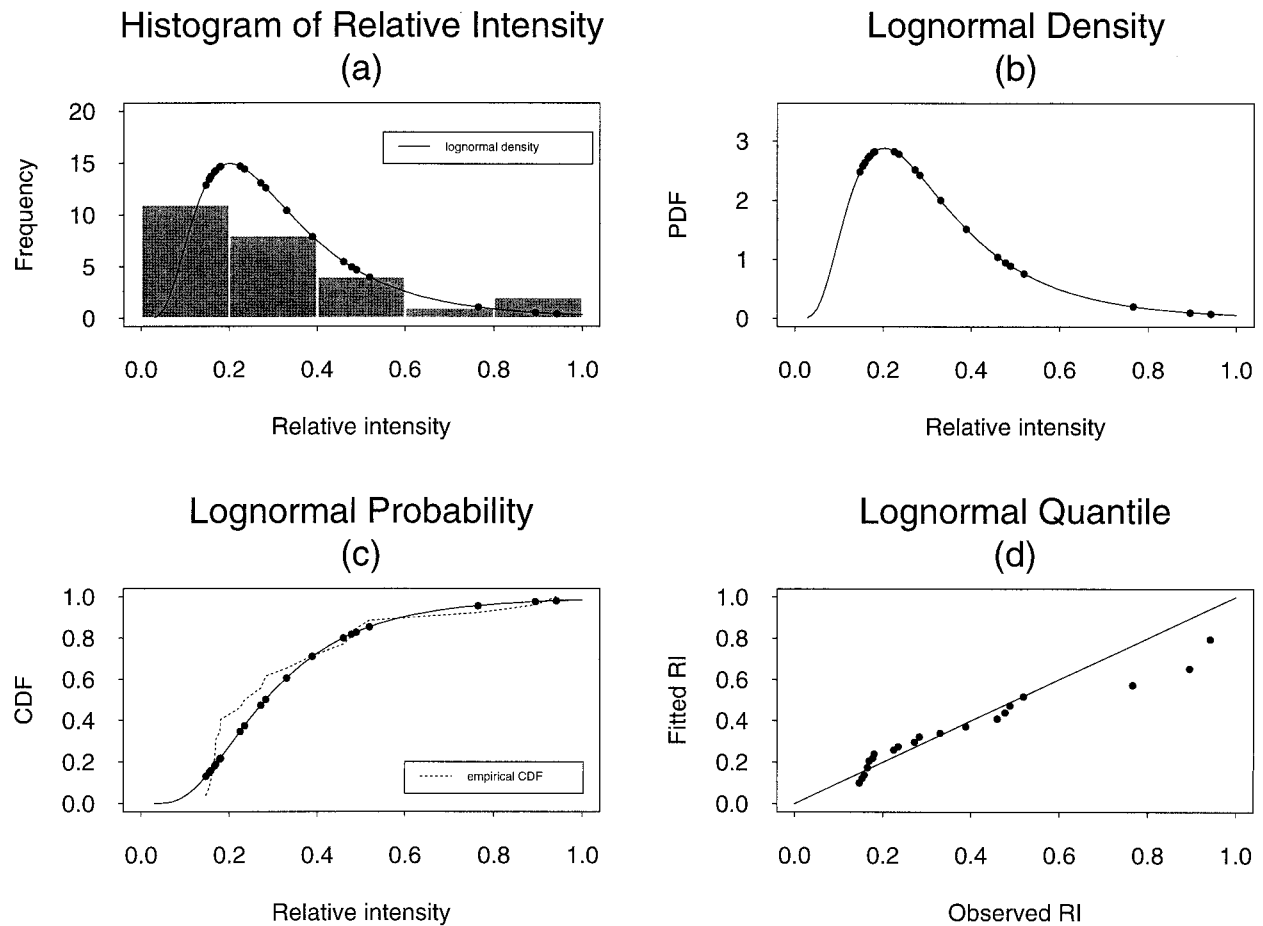


FIG. 6. (a) Histogram, (b) pdf, (c) CDF and (d) $Q-Q$ plots of the relative intensity of tropical cyclones for the lognormal distribution. The dots are for 26 tropical cyclones in the vicinity of Hawaii. In (c) the solid and dashed curves denote the theoretical and empirical CDF, respectively. In the $Q-Q$ plot, observed RIs are on the horizontal and the fitted RIs are on the vertical. The diagonal line indicates 1:1 correspondence.

oretical CDFs or between the observed RIs and fitted RIs as the test statistic. The results are shown in the sixth and seventh columns in Table 2. The lognormal distribution is best for the overall goodness of fit because the discrepancy is smallest. Therefore, the lognormal distribution is used in the Monte Carlo method to simulate the RIs and to estimate the probabilities and return periods of tropical cyclone intensities.

c. An improved estimate of the return periods of tropical cyclone intensities

The Monte Carlo simulation, in essence, is a data generation technique used to simulate the random process by a computer random number generator (e.g., Chu 1995). It is often used to find empirical solutions to rather complex mathematical problems. One recent ap-

TABLE 2. Parameters and goodness of fit of tropical cyclone data for the Gumbel, Weibull, and lognormal distributions. Rows 2, 3, and 4 correspond to the entire 47-yr dataset (1949–95). Rows 5, 6, and 7 correspond to the satellite era data (1970–95).

| | Distribution | Parameter 1 | Parameter 2 | D value | Avg CDF difference | Avg quantile difference |
|----------------------------|--------------|-------------------|-------------------|---------|--------------------|-------------------------|
| 1949–95 (Full dataset) | Gumbel | $\xi = 0.2343$ | $\beta = 0.1787$ | 0.1589 | 0.0679 | 0.0554 |
| | Weibull | $\alpha = 1.6585$ | $\beta = 0.3815$ | 0.1488 | 0.0713 | 0.0573 |
| | Lognormal | $\mu = -1.2645$ | $\sigma = 0.5804$ | 0.1699 | 0.0623 | 0.0470 |
| 1970–95 (Satellite era) | Gumbel | $\xi = 0.2043$ | $\beta = 0.1709$ | 0.1970 | 0.0916 | 0.0688 |
| | Weibull | $\alpha = 1.6052$ | $\beta = 0.3423$ | 0.1770 | 0.0930 | 0.0695 |
| | Lognormal | $\mu = -1.3685$ | $\sigma = 0.5592$ | 0.2072 | 0.0690 | 0.0519 |

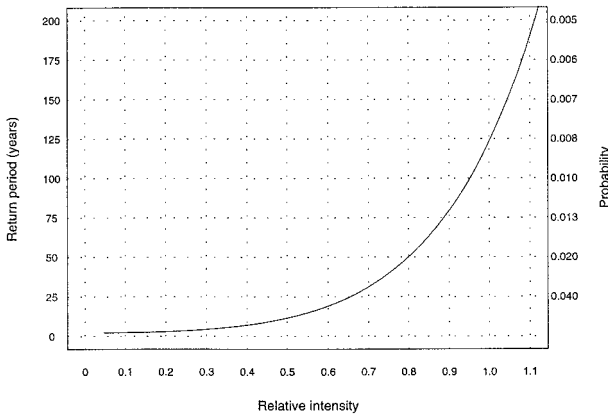


FIG. 7. Same as Fig. 5 except for 1000 simulated relative intensities.

plication of the Monte Carlo simulation to the tropical cyclone-related research can be found in Chu and Wang (1997) in that a two-sample permutation procedure is used to conduct hypothesis testing to determine whether the difference in tropical cyclone incidences between El Niño and non-El Niño batches is significant. Through the Monte Carlo simulation, a large number of RIs ($n = 1000$) can be simulated from (19) based on the lognormal distribution with the fitted parameters presented in Table 2. Using the simulated RIs to (11) and (12), an estimate of the probabilities and return periods of tropical cyclone intensities in the vicinity of Hawaii can be obtained. The results are given in Fig. 7.

For any tropical cyclone with a given maximum RI, one can obtain its return period from Fig. 7. For example, the return period is about 50 years for a tropical cyclone with RI equal to or greater than 0.8 within 250 n mi of Honolulu. Figure 7 is based on the assumption that the data follow the fitted lognormal distribution; thus, the result is different from Fig. 5, which is based on little available data. Figure 5 can be used only in the observed data range, but Fig. 7 can be extended to estimate the return periods of any potentially strong tropical cyclones. However, caution must be exercised in estimating the return periods at the longer timescales. Kangieser (1994) recommended that return periods should be extrapolated only to about two or three times the sample size due to the uncertainties introduced by the finite sample size.

Because the primary source of hurricane-related damages in Hawaii is wind, the simulated RIs are converted back to central pressures, then to gradient winds and maximum wind speeds by applying (2), (3), and (4). Replacing RIs in (11) and (12) with the converted maximum wind speeds, the probabilities and return periods of the maximum wind speeds based on the lognormal are presented in Fig. 8 (solid line). The results are slightly different from those in Fig. 7 because a simple linear relation between RIs and maximum wind speeds does not exist. The return periods derived from the Weibull (dashed line) and Gumbel (sparse dashed line) distri-

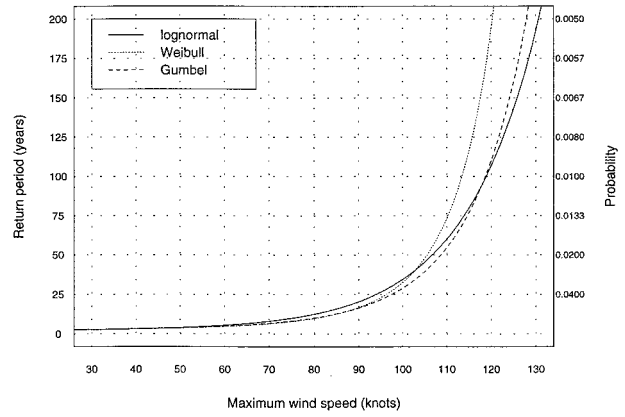


FIG. 8. Same as Fig. 5 except for the maximum wind speeds associated with each of 1000 simulated relative intensities. The sparse dashed, dashed, and solid lines are the return periods derived from the Gumbel, Weibull, and lognormal distributions, respectively.

butions are also shown in Fig. 8. The results for the maximum wind speeds less than 100 kt are similar for the three distributions. The differences increase with the increasing maximum wind speeds.

Table 3 lists the returns periods of the maximum wind speeds equal to or greater than 34, 50, 64, 80, 100, 110, and 125 kt, based on the lognormal shown in Fig. 8. These selected speeds are deemed relevant to civil planning and disaster preparedness. Here, 34 kt is the minimal tropical storm intensity; 50 kt might be considered as the threshold value of destructive winds; 64 kt is the minimal hurricane intensity. Maximum wind speeds of 80, 100, 110, and 125 kt were observed or estimated during Hurricanes Iwa, Fico, Dot, and Iniki, respectively. Nina is not considered here because its maximum wind speed (75 kt) is too close to Iwa (80 kt). The return periods for the aforementioned seven selected maximum wind speeds are estimated to be 3.2, 4, 6.6, 12, 33, 59, and 137 years (second column in Table 3). For the other weaker tropical cyclones, the return periods are from about 2 to 10 years.

TABLE 3. Maximum wind speeds and their corresponding return periods. The first column gives the maximum wind speeds in kt. The second and third columns give the return periods estimated from the entire 47-yr dataset (1949–95) and the satellite era data (1970–95), respectively.

| Selected max wind speed (kt) | 1949–95 (Full dataset) | 1970–95 (Satellite era) |
|------------------------------|------------------------|-------------------------|
| 34 | 3.2 | 3.2 |
| 50 | 4 | 4 |
| 64 | 6.6 | 6.6 |
| 80 | 12 | 13 |
| 100 | 33 | 42 |
| 110 | 59 | 81 |
| 125 | 137 | 202 |

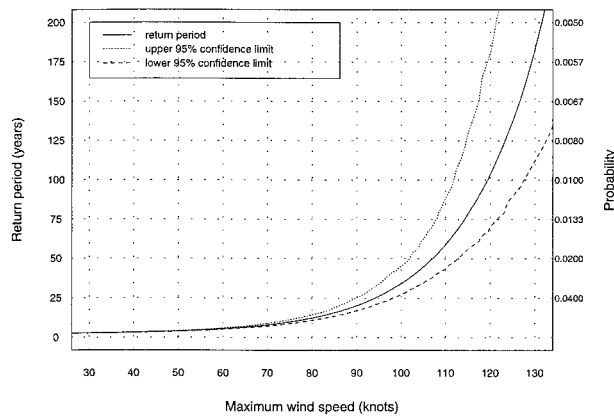


FIG. 9. The 95% confidence intervals of the return periods for the maximum wind speeds associated with the 1000 simulated relative intensities based on the lognormal distribution.

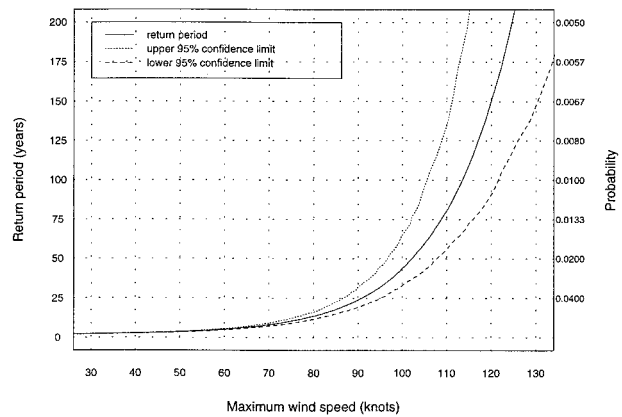


FIG. 10. Same as Fig. 9 except for the satellite era (1970–95).

d. An estimate of the confidence intervals of return periods

Based on the lognormal distribution, 500 batches of the simulated RIs are generated by the Monte Carlo method. Each batch consists of 1000 RIs. The RIs are converted back to maximum wind speeds. For each batch of 1000 maximum wind speeds, one batch of 1000 return periods can be estimated. Thus, 500 batches, each consisting of 1000 return periods, are obtained to construct the empirical distribution of the return periods. For each of 1000 maximum wind speeds, 500 return periods can be obtained. For the batches of 500, the 95% confidence interval is simply between the smallest 13 and largest 13 return periods of the maximum wind speed (the so-called percentile method).

Figure 9 shows the upper (dashed line) and lower (sparse dashed line) 95% confidence limits of the return periods (solid line) for a range of maximum wind speeds associated with tropical cyclones in the vicinity of Hawaii. As shown in Table 3, the return period for the maximum wind speed, which is of at least Iniki's intensity (125 kt), is estimated to be 137 years. The return periods are 59, 33, and 12 years for the maximum wind speeds, which correspond to at least Dot's (110 kt), Fico's (100 kt), and Iwa's (80 kt) intensities. The 95% confidence intervals range from about 88 to 250 years for the return period of 137 years, 43 to 71 years for the return period of 59 years, 26 to 44 years for the return period of 33 years, 10.5 to 14 years for the return period of 12 years (Fig. 9). The width of the confidence interval naturally increases with the increasing wind speed.

5. Sensitivity test

The study so far conducted is based on the entire 47-yr dataset from 1949 to 1995. The data qualities of the tropical cyclones may be questionable during the presatellite era (1949–69). To examine the sensitivity of

the results presented earlier, the presatellite era is removed. Accordingly, the data from 1970 to 1995 are refitted with the Gumbel, Weibull, and lognormal distributions.

Table 2 lists the parameters of the three distributions, *D* values, average CDF differences, and average quantile differences between the theoretical and empirical distributions. Although the parameters are all slightly different with or without the presatellite era data, the smallest average CDF and quantile differences are always found in the lognormal distribution. Therefore, the lognormal appears to be the best distribution even when the presatellite era is removed from the full dataset.

The return periods and their 95% confidence intervals of the maximum wind speeds associated with tropical cyclones are estimated based on the lognormal distribution via the Monte Carlo method using the data from 1970 to 1995. The results are shown in Fig. 10 and the third column of Table 3. A comparison between columns 2 and 3 in Table 3 indicates that the return periods are almost the same when the maximum wind speeds are not greater than 80 kt. The 95% confidence intervals are also very close to each other, as shown in Figs. 9 and 10 for the above intensities. However, the differences increase as maximum wind speeds increase because of the rareness of the strong hurricanes in the vicinity of Hawaii. For the maximum wind speed at 125 kt or greater, which is observed during Iniki, the return period is estimated as about 202 years (Fig. 10). Note that this estimate is still within the 95% confidence intervals of the return period of 137 years, as shown in Fig. 9 (88–250 years).

6. Summary

Assessing the vulnerability of a specific region to tropical cyclones is an important first step in disaster prevention plans. Therefore, a climate risk assessment involving maximum wind speeds associated with tropical cyclones is conducted and this climate information is of particular interest to government agencies, public

interest groups, and private sectors. In this study, tropical cyclones in the vicinity of Hawaii have been identified from historical records and a relatively advanced methodology has been developed to estimate the return period of exceeding a given maximum wind speed associated with a tropical cyclone.

A dimensionless quantity, called relative intensity, is efficiently used in the extreme value distributions because of its compact representativeness of tropical cyclone characteristics and its desirable range, usually between 0 and 1. The three extreme value distributions, Gumbel, Weibull, and lognormal, each describe tropical cyclone intensities well. Among them, the lognormal distribution appears to possess the best overall goodness of fit. The main results are listed in Table 3 and are shown in Figs. 7–10. The return period of maximum wind speeds equal to or greater than 125 kt, which occurred during Iniki, is estimated to be 137 years, and its true value lies in the interval between 88 and 250 years with 95% confidence. For the other less strong but nevertheless menacing hurricanes (e.g., Dot, Fico, and Iwa), the return periods of maximum wind speeds equal or exceeding 110, 100, and 80 kt are estimated to be 59, 33, and 12 years, respectively. Because the sample size (47 years) in this study is finite, estimates of return periods of tropical cyclone winds with periods beyond two to three times the actual sample size should be held in caution.

The sensitivity test has been conducted by removing the presatellite era data. Estimates of return periods are not very sensitive to the varying data length, particularly in the range when tropical cyclone intensities are not too strong. Results of this study may provide a relatively reasonable and consistent basis for making realistic decisions concerning disaster mitigation of tropical cyclone hazards in the vicinity of Hawaii. It is hoped that the methodology developed and results presented here would be of value to other tropical cyclone-prone regions (e.g., Fiji) in their disaster prevention plans. Finally, the applications of the methodology in this study are not only limited to tropical cyclones but may also extend to estimating return periods of other natural disasters such as flash floods and earthquakes.

Acknowledgments. We would like to thank T. Schroeder, S. Businger, and G. Barnes for their helpful comments and suggestions; Z.-P. Yu for providing the tropical cyclone data; and G. Trapp of the former Central Pacific Hurricane Center of the National Weather Service (NWS) in Honolulu for his encouragement on this research topic. Comments made by an anonymous reviewer were helpful. This study has been funded by the Federal Emergency and Management Agency via Hawaii State Civil Defense. JXW was supported by the NWS Pacific fellowship to the Department of Meteor-

ology at the University of Hawaii through a NOAA cooperative agreement.

REFERENCES

- Batts, M., M. Cordes, L. Russell, J. Shaver, and E. Simiu, 1980: Hurricane wind speeds in the United States. NBS Building Science Series, No. 124, 41 pp.
- Brown, B. G., and R. W. Katz, 1995: Regional analysis of temperature extremes: Spatial analog for climate change? *J. Climate*, **8**, 108–119.
- Chu, P.-S., 1995: Hawaii rainfall anomalies and El Niño. *J. Climate*, **8**, 1697–1703.
- , and J. Wang, 1997: Tropical cyclone occurrences in the vicinity of Hawaii: Are the differences between El Niño and non-El Niño years significant? *J. Climate*, **10**, 2683–2689.
- Darling, R. W. R., 1991: Estimating probabilities of hurricane wind speeds using a larger-scale empirical model. *J. Climate*, **4**, 1035–1046.
- Emanuel, K. A., 1988a: Toward a general theory of hurricanes. *Amer. Sci.*, **76**, 370–379.
- , 1988b: The maximum intensity of hurricanes. *J. Atmos. Sci.*, **45**, 1143–1155.
- Georgiou, P. N., 1985: Design wind speeds in tropical cyclone-prone regions. Ph.D. thesis, University of Western Ontario, 295 pp.
- Gumbel, E. L., 1958: *Statistics of Extremes*. Columbia University Press, 375 pp.
- Haan, C. T., 1977: *Statistical Methods in Hydrology*. Iowa State University Press, 378 pp.
- He, Y., and A. G. Barnston, 1996: Long-lead forecasts of seasonal precipitation in the tropical Pacific islands using CCA. *J. Climate*, **9**, 2020–2035.
- Jordan, C. L., 1961: Marked changes in the characteristics of the eye of intense typhoons between the deepening and filling stages. *J. Meteor.*, **18**, 779–789.
- Kangieser, P. C., 1994: Estimating the likelihood of extreme events. *Weatherwise*, **47**, 38–40.
- Landsea, C. W., and W. M. Gray, 1992: The strong association between western Sahelian monsoon rainfall and intense Atlantic hurricanes. *J. Climate*, **5**, 435–453.
- Lowery, M. D., and J. E. Nash, 1970: A comparison of methods of fitting the double exponential distribution. *J. Hydrol.*, **10**, 259–275.
- Neumann, C. J., 1987: The National Hurricane Center Risk Analysis Program (HURISK). NOAA Tech. Memo. NWS NHC 38, 56 pp.
- Ramage, C. S., 1995: Forecasters guide to tropical meteorology. AWS/TR-95/001, 392 pp. [Available from Air Weather Service, 102 West Losey St., Scott Air Force Base, IL 62225.]
- Rosendal, H. E., and S. L. Shaw, 1982: Relationships of maximum sustained winds to minimum sea level pressure in central north Pacific tropical cyclones. NOAA Tech. Memo. NWSTM PR-24, 18 pp.
- Rupp, J. A., and M. A. Lander, 1996: A technique for estimating recurrence intervals of tropical cyclone-related high wind in the tropics: Results for Guam. *J. Appl. Meteor.*, **35**, 627–637.
- Russell, L. J., 1971: Probability distributions for hurricane effects. *J. Waterw. Harbors Coastal Eng. Div. Amer. Soc. Civ. Eng.*, **97**, 139–154.
- Schwerdt, R. W., F. P. Ho, and R. R. Watkins, 1979: Meteorological criteria for standard project hurricane and probable maximum hurricane windfield, gulf and east coasts of the United States. NOAA Tech. Rep. NWS 23, 317 pp.
- Wilks, D. S., 1995: *An Introduction to Statistical Methods in the Atmospheric Sciences*. Academic Press, 465 pp.
- Willoughby, H. E., 1990: Gradient balance in tropical cyclones. *J. Atmos. Sci.*, **47**, 265–274.
- Zhang, G. J., V. Ramanathan, and M. J. McPhaden, 1995: Convection–evaporation feedback in the equatorial Pacific. *J. Climate*, **8**, 3040–3051.